

# SCIENTIFIC REPORTS



OPEN

## Peroxisome Proliferator-Activated Receptor gamma negatively regulates liver regeneration after partial hepatectomy via the HGF/c-Met/ERK1/2 pathways

Zhangjun Cheng<sup>1,2</sup>, Lei Liu<sup>1,3</sup>, Xue-Jun Zhang<sup>1,4</sup>, Miao Lu<sup>1,2</sup>, Yang Wang<sup>1,2</sup>, Volker Assfalg<sup>1</sup>, Melanie Laschinger<sup>1</sup>, Guido von Figura<sup>5</sup>, Yoshiaki Sunami<sup>1,6</sup>, Christoph W. Michalski<sup>1,6</sup>, Jörg Kleeff<sup>1,6</sup>, Helmut Friess<sup>1</sup>, Daniel Hartmann<sup>1</sup> & Norbert Hüser<sup>1</sup> 

Peroxisome Proliferator-Activated Receptor gamma (PPAR $\gamma$ ) is a nuclear receptor demonstrated to play an important role in various biological processes. The aim of this study was to determine the effect of PPAR $\gamma$  on liver regeneration upon partial hepatectomy (PH) in mice. Mice were subjected to two-thirds PH. Before surgery, mice were either treated with the PPAR $\gamma$  agonist rosiglitazone, the PPAR $\gamma$  antagonist GW9662 alone, or with the c-met inhibitor SGX523. Liver-to-body-weight ratio, lab values, and proliferation markers were assessed. Components of the PPAR $\gamma$ -specific signaling pathway were identified by western blot and qRT-PCR. Our results show that liver regeneration is being inhibited by rosiglitazone and accelerated by GW9662. Inhibition of c-Met by SGX523 treatment abrogates GW9662-induced liver regeneration and hepatocyte proliferation. Hepatocyte growth factor (HGF) protein levels were significantly downregulated after rosiglitazone treatment. Activation of HGF/c-Met pathways by phosphorylation of c-Met and ERK1/2 were inhibited in rosiglitazone-treated mice. In turn, blocking phosphorylation of c-Met significantly abrogated the augmented effect of GW9662 on liver regeneration. Our data support the concept that PPAR $\gamma$  abrogates liver growth and hepatocellular proliferation by inhibition of the HGF/c-Met/ERK1/2 pathways. These pathways may represent potential targets in response to liver disease and could impact on the development of molecular therapies.

The liver has a unique capability of precisely regulating compensatory hypertrophy and hyperplasia to restore the loss of functional mass. Various studies on liver regeneration induced by two-thirds PH have studied the complex network of signaling pathways leading to liver regeneration, including various cytokines, responsible for hepatocyte priming; growth factors, responsible for cell cycle progression; hormones and energy metabolism<sup>1-4</sup>. However, accurate mechanisms of liver regeneration are still incompletely determined.

Peroxisome Proliferator-Activated Receptor gamma (PPAR $\gamma$ ), a member of the nuclear receptor superfamily, is one of the nuclear transcription factors which responds to its natural and/or synthetic ligands<sup>5</sup>. A number of studies have revealed that PPAR $\gamma$  participates in a large variety of biological processes, including metabolism, anti-inflammation, cell cycle, and cell differentiation, as well as immunoregulation<sup>6-8</sup>. In recent years, several studies have determined that PPAR $\gamma$  is involved in tumorigenesis and organ development, it leads to cell cycle arrest, promotes cell differentiation, inhibits angiogenesis, and induces apoptosis<sup>9-12</sup>. The cell cycle regulation

<sup>1</sup>Technical University of Munich, School of Medicine, Klinikum rechts der Isar, Department of Surgery, Munich, 81675, Germany. <sup>2</sup>Department of General Surgery, Zhongda Hospital, Southeast University, Nanjing, 210009, China. <sup>3</sup>Department of Spine Surgery, Zhongda Hospital, Southeast University, Nanjing, 210009, China. <sup>4</sup>Department of Orthopedic Surgery, Zhongda Hospital, Southeast University, Nanjing, 210009, China. <sup>5</sup>Technical University of Munich, School of Medicine, Klinikum rechts der Isar, II. Medical Clinic and Polyclinic, Munich, D-81675, Germany. <sup>6</sup>Department of Surgery, University Clinic Halle (Saale), Martin-Luther-University Halle-Wittenberg, Halle (Saale), 06097, Germany. Zhangjun Cheng, Lei Liu, Xue-Jun Zhang, Daniel Hartmann and Norbert Hüser contributed equally to this work. Correspondence and requests for materials should be addressed to N.H. (email: [norbert.hueser@tum.de](mailto:norbert.hueser@tum.de))

properties of PPAR $\gamma$  have encouraged pursuing new functions in liver regeneration. Some studies have shown that activation of PPAR $\gamma$  by thiazolidinediones can inhibit liver regeneration<sup>13,14</sup>. In addition, another study revealed that metabolic and hepatocellular proliferative responses to PH are modestly augmented in liver-specific PPAR $\gamma$  null mice<sup>15</sup>. These observations indicate that PPAR $\gamma$  does play an important role during liver regeneration although the underlying molecular mechanisms remain unclear, which encouraged us to evaluate the influence of PPAR $\gamma$  on liver regeneration after surgical resection and treatment with the PPAR $\gamma$  agonist rosiglitazone, the PPAR $\gamma$  antagonist GW9662 alone, or together with the c-met inhibitor SGX523.

In the present study, we identified a novel effect of PPAR $\gamma$  on hepatectomized mice that is mediated by regulating the activation of HGF/c-Met/ERK1/2 pathways. We showed that regulation of HGF signaling provides additional new insights on the role of PPAR $\gamma$  in the delay of liver regeneration in response to liver resection.

## Materials and Methods

**Animals and surgery.** Eight to ten week-old female C57BL/6J mice (Charles River laboratory) were maintained under a standard 12-hour-light/dark cycle with free access to standard mouse chow and tap water before and after surgery. 70% PH was performed as described previously under general anesthesia with inhaled isoflurane ( $n = 4-6$  for each time point and for each treatment group)<sup>16</sup>. Briefly, the left and median lobes of the liver were ligated and resected after mid-ventral laparotomy. Mortality rate was less than 5%.

In order to evaluate the effect of PPAR $\gamma$  on liver regeneration in this PH mouse model, we treated mice either with 20 mg/kg body weight rosiglitazone (Glaxo SmithKline) by oral gavage or with 10 mg/kg body weight GW9662 (M6191, Sigma Aldrich) by intraperitoneal injection 2 days before surgery, respectively. To further investigate the underlying mechanism of PPAR $\gamma$  on liver regeneration, two other groups of mice were treated with 25 mg/kg body weight SGX523 (Selleck) by oral gavage beginning at the operative day and a concentration of 0.2% fenofibrate mixed with chow food beginning 5 days before PH. All treatments continued until the time of animal sacrifice and tissue harvest.

For sample collection, necropsy was carried out immediately after euthanasia. Removed liver lobes were immediately weighed, snap-frozen in liquid nitrogen, and stored at  $-80^{\circ}\text{C}$  for subsequent genomic and proteomic analyses.

All animal experimental procedures were carried out under a protocol approved by the animal studies committee of the Technische Universität München and the government of Oberbayern (TVA AZ: 55.2-1-54-2532-66-12) and were in accordance with institutional guidelines.

**Biochemistry analysis.** Serum aminotransferase activity, glucose, cholesterol, and triglyceride were determined by our hospital's clinical laboratory.

**Histology and immunohistochemistry.** Liver tissue was fixed overnight in 4% PFA, embedded in paraffin, and sectioned in 3  $\mu\text{m}$  slices. immunohistochemistry (IHC) was performed with the following antibodies: anti-Ki67 antibody (1:500, Cell Signaling Technology), anti-PH3 antibody (1:400, Cell Signaling Technology), and anti-PPAR $\gamma$  antibody (1:1000, Cell Signaling Technology). They all were counterstained with hematoxylin and eosin (H&E). Hepatocyte proliferation was determined by quantification of Ki67- and PH3-positive cells. The percentage of proliferative hepatocyte was determined by examination of at least four random 100x fields in three different sections. At least 200 nuclei were counted in each field. For morphology assessment, the sections were also stained with H&E.

**Real-time quantitative PCR.** Total RNA was isolated from liver tissue using an RNeasy Mini Kit (QIAGEN) according to the manufacturer's instruction and single strand cDNA was synthesized from 800 ng of total RNA using a QuantiTect Kit (QIAGEN). For each gene analyzed, a 5  $\mu\text{l}$  aliquot of cDNA was added to a reaction mixture containing gene-specific primers (Supplementary Table 1), deoxynucleotides, and SYBR Green I. The Real-time quantitative PCR was performed using a LightCyclerR 480 real-time PCR machine. The relative amounts of the mRNA studied by means of the  $2^{-\Delta\Delta\text{CT}}$  method.

**Western blot.** All liver tissue lysates were made from snap-frozen liver tissue using RIPA buffer (Cell Signaling Technology), homogenates were spun at 13,000 g for 20 minutes at  $4^{\circ}\text{C}$  to remove cell debris. Twenty-microgram aliquots of protein lysate were subjected to SDS-PAGE, followed by transfer onto nitrocellulose membrane and incubated with anti-PPAR $\gamma$  (E-8) (Santa Cruz); anti-phospho STAT3 (Tyr705), anti-STAT3, anti-cyclin D1, anti-phospho ERK (Tyr202/204), anti-ERK, anti-phospho c-Met (Tyr1234/1235), and anti-c-Met (all from Cell Signaling Technology); anti-HGF (Novus Biologicals); anti-PPAR $\alpha$  (abcam); and anti-GAPDH, anti- $\beta$ -actin (Santa Cruz). Then the membranes were incubated with a horseradish peroxidase-conjugated secondary antibody and developed using the enhanced chemiluminescence system (Amersham).

**Statistics.** All experiments were performed in triplicates and the data shown are representative of results consistently observed. Quantitative data was presented as means  $\pm$  standard deviation. Multiple comparisons were performed by one-way analysis of variance (ANOVA) with repeated measures, followed by a *post hoc* Fisher's least significant differences test. Statistical significance was set at  $p < 0.05$ . Differences in diagrams that are not marked with asterisks are not significantly different. All statistics were performed using SPSS 13.0 (SPSS Inc., Chicago, IL, USA).

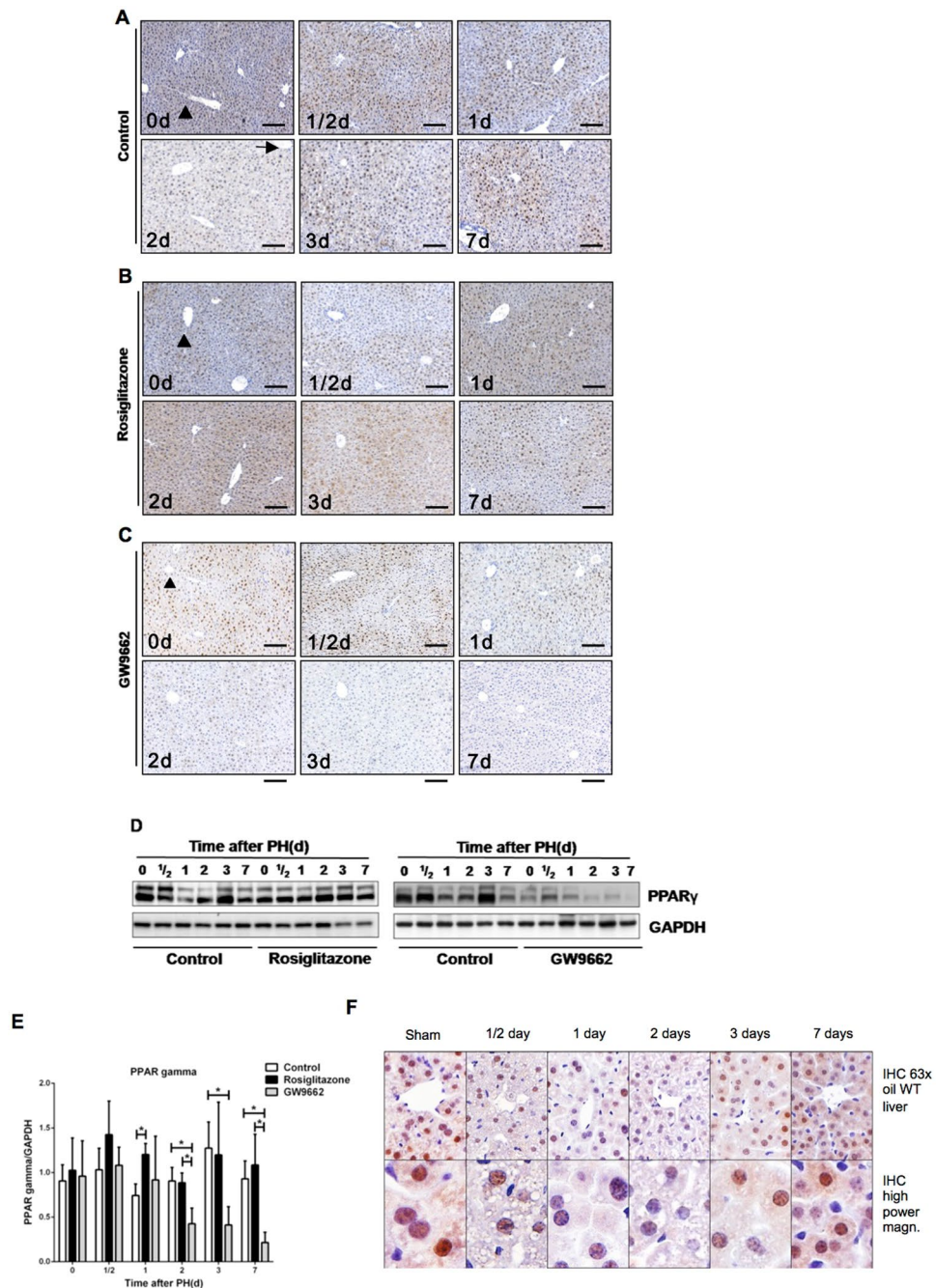


**Figure 1.** PPAR $\gamma$  inhibits hepatocellular proliferation during mouse liver regeneration (A) Hepatic PPAR $\gamma$  expression during mouse liver regeneration. Representative Immunohistochemistry (IHC) analysis for PPAR $\gamma$  in untreated mice, (B) rosiglitazone-treated mice, and (C) GW9662-treated mice at different time points after PH. Scale bar: 200  $\mu$ m. Arrow: Centrilobular zone, Arrowhead: Periportal zone. (D) Hepatic expression of PPAR $\gamma$  protein in control mice, rosiglitazone-treated mice and GW9662-treated mice at different time points after partial hepatectomy. (E) Quantification of Western blots after analysis of three biological triplicates. (F) Analysis of cellular localization of PPAR gamma at different time points after PH in wild type mice. \* $p < 0.05$ .

## Results

**PPAR $\gamma$  inhibits hepatocellular proliferation during mouse liver regeneration.** At first, the expression pattern of PPAR $\gamma$  in response to PH was examined (Fig. 1A–C). In the liver of untreated mice, IHC revealed a strong staining in hepatocytes, especially in the nuclei at 0h time point. The distribution of PPAR $\gamma$  in the liver has its own characteristic, namely that PPAR $\gamma$  is predominantly expressed in the centrilobular zone (marked by arrow) but weakly in the periportal zone (marked by arrowhead). The expression of PPAR $\gamma$  was markedly reduced during the early phase of liver regeneration (12–48 hours following PH) and recovered gradually during the late phase of regeneration (3–7 days following PH). Protein expression of PPAR $\gamma$  showed a tendency consistent with

the previously described IHC results (Fig. 1D). An analysis of cellular localization of PPAR $\gamma$  at different time points after PH in wild type mice showed that PPAR $\gamma$  can be found in the cytosol and in the nucleus but was increasingly relocalized from the cytosol to the nucleus over time after PH (Fig. 1F). To investigate the role of PPAR $\gamma$  in regulating hepatocyte proliferation, we treated mice with a PPAR $\gamma$  agonist (rosiglitazone) and a PPAR $\gamma$  antagonist (GW9662) prior to PH. The expression of PPAR $\gamma$  was maintained during the whole process of liver regeneration in rosiglitazone-treated mice and significantly higher compared to untreated mice at 24 hours after PH ( $p < 0.05$ , Fig. 1B,D,E). In contrast, PPAR $\gamma$  expression decreased gradually in GW9662-treated mice and was significantly lower compared to untreated mice at 2 days, 3 days and 7 days after PH ( $p < 0.05$ , Fig. 1C–E).

**Ligand activation of PPAR $\gamma$  inhibits mouse liver regeneration after PH.** Next, we studied PH-induced liver regeneration in untreated, rosiglitazone-treated, and GW9662-treated mice. The liver to body weight ratio (the weight of the remnant liver divided by the initial body weight) rose sharply between 1 to 3 days (from 3.19% to 3.79%), and regained almost preoperative values at day 7 after PH in the control group (Fig. 2A). In contrast, rosiglitazone-treated mice displayed significantly delayed gain in liver mass compared to untreated mice on day 1, day 2, and day 3 post-PH, whereas the ratio increased in a significantly accelerated way in GW9662-treated mice on day 3 post-PH ( $p < 0.05$ , Fig. 2A). Despite showing a delayed/accelerated rate of liver regeneration over the course of time, the final mass of the remnant liver in each group showed no significant difference compared to the control group on day 7 and day 14 after PH (Fig. 2A and data not shown).

In order to investigate the effects of PPAR $\gamma$  on hepatocyte proliferation and cell cycle entry in response to PH, we performed IHC for Ki67 and PH3 as well as western blot and qRT-PCR analysis for cyclin D1 in liver tissue. Consistent with previous studies, the results showed that Ki67-positive and PH3-positive hepatocytes peaked at day 2 post-PH in untreated mice (Fig. 2B–D)<sup>17</sup>. Compared to untreated mice, the number of Ki67- and PH3-positive hepatocytes was found to be decreased and delayed in rosiglitazone-treated mice but significantly increased in GW9662-treated mice at day 2 post-PH ( $p < 0.05$ , Fig. 2B–D). In line with these observations, induction of cyclin D1, a key mediator of cell cycle progression at G1 and G1/S phase of the cell cycle, was significantly attenuated at 12 hours post-PH in the rosiglitazone-treated mice as compared to untreated and GW9662-treated mice ( $p < 0.05$ , Fig. 2E–G). In accordance with these results, qRT-PCR examination of cyclin B1 gene expression also revealed significantly reduced levels in rosiglitazone-treated mice compared to untreated and GW9662-treated mice at day 2 post-PH ( $p < 0.05$ , Supplementary Figure 1). These data demonstrate that PPAR $\gamma$  activation inhibits liver regeneration at least partly by controlling hepatocyte proliferation.

We also examined liver function in untreated, rosiglitazone-treated and GW9662-treated mice after PH. H&E staining and serum biochemistry analyses revealed that no mouse exhibited histological alterations or abnormal metabolic parameters characteristic for drug-induced hepatic injury at day 7 post-PH (Supplementary Figures 2A and B). A slight ALT and AST elevation could be seen in rosiglitazone-treated mice compared to untreated and GW9662-treated mice at 12 hours post-PH with normal values in all three groups at around 24 hours post-PH and thereafter (Supplementary Figure 2B).

**PPAR $\alpha$  activation does not influence hepatic regeneration following PH.** PPARs are known to exist in three isoforms ( $\alpha$ ,  $\beta$ ,  $\gamma$ ). To address whether rosiglitazone-activated PPAR $\gamma$  is specific to influence hepatocyte proliferation after PH, the PPAR isoform  $\alpha$  was activated by fenofibrate treatment. Even though there was a significant increase in the liver to body weight ratio in fenofibrate-treated mice compared to untreated mice at 2 days and 3 days post-PH ( $p < 0.05$ , Fig. 3A), up-regulation of PPAR $\alpha$  did not have any influence on the number of Ki67 and PH3-positive hepatocytes in fenofibrate-treated mice compared to untreated mice at day 2 and day 3 post-PH (Fig. 3B–E). These results indicate that, in contrast to rosiglitazone-activated PPAR $\gamma$ , fenofibrate-activated PPAR $\alpha$  in the liver is incapable of regulating liver regeneration in a PH model.

**PPAR $\gamma$  does not impair the initiation of mouse liver regeneration.** PPAR $\gamma$  activation is known to inhibit TNF $\alpha$  production in human neural stem cells<sup>18</sup>. During liver regeneration, the TNF $\alpha$ /IL6/STAT3 signaling pathways plays a pivotal role in maintaining the viability of hepatocytes and enhancing their responsiveness to growth factors. To gain insight in the molecular pathways of PPAR $\gamma$  function in the liver, we examined whether PPAR $\gamma$  activation inhibits liver regeneration via decreased TNF $\alpha$ /IL6 production. The hepatic mRNA levels of TNF $\alpha$  and IL6 were increased in untreated mice, rosiglitazone-treated mice, and GW9662-treated mice 12 hours after PH. However, neither 0 hours nor 12 hours after PH any significant difference could be observed between these three different groups (Supplementary Figure 3A and B). Similarly, an induction of phosphorylated STAT3 was observed in all groups 12 hours after surgery, however, no difference in both the magnitude and the kinetics of IL-6-induced STAT3 phosphorylation could be ascertained between untreated mice, rosiglitazone-treated mice, and GW9662-treated mice at any time point (Supplementary Figure 3C and D). Taken together, these results indicate that an altered expression of PPAR $\gamma$  is dispensable for the control of the TNF $\alpha$ /IL6/STAT3 signaling pathways during liver regeneration.

**PPAR $\gamma$  inhibits the activation of HGF/c-Met/ERK1/2 signaling pathways in the regenerating liver.** HGF is considered as an extremely important growth factor that promotes hepatocyte proliferation following PH<sup>19</sup>. To gain further insight into the underlying mechanisms, we investigated whether altered expression of PPAR $\gamma$  regulates HGF/c-Met/ERK1/2 signaling after PH. Following PH, HGF and HGF-induced phosphorylation of c-Met were dramatically increased over 12 hours and maintained high until 3 days after PH in each group (Fig. 4). As compared with untreated mice, the level of HGF activity was significantly lower in rosiglitazone-treated mice 24 hours post-PH ( $p < 0.05$ ) and resulted in a decreased activation of c-Met (Tyr1234/1235). These results demonstrate that ligand activation of PPAR $\gamma$  significantly down-regulates HGF

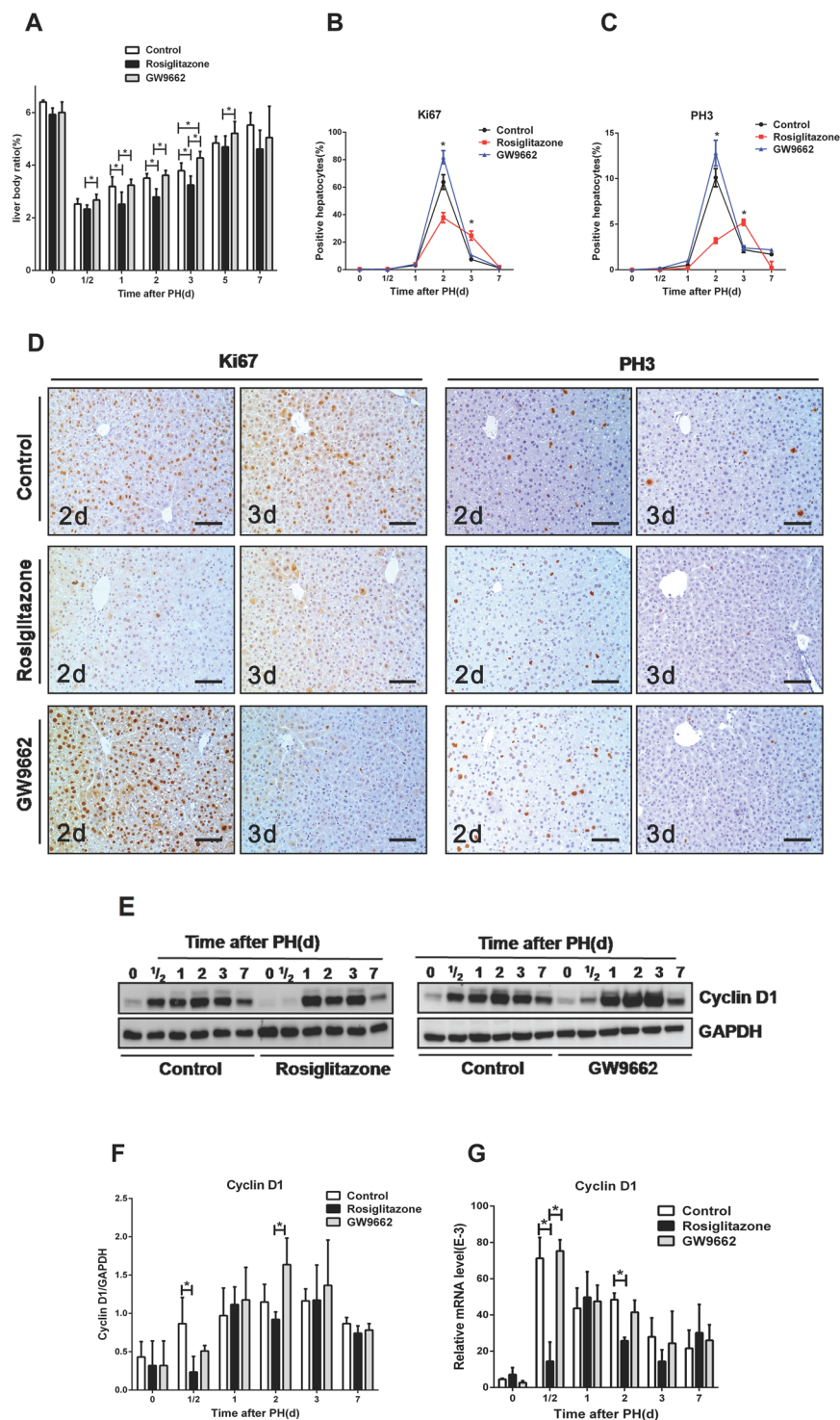


**Figure 2.** Ligand activation of PPAR $\gamma$  inhibits mouse liver regeneration after PH. **(A)** Liver to body weight ratio in untreated mice, rosiglitazone-treated mice, and GW9662-treated mice at different time points after PH. **(B)** Quantification of Ki67-positive hepatocytes and **(C)** PH3-positive hepatocytes. **(D)** Micrographs of liver sections immunostained with Ki67 & PH3 antibody from untreated, rosiglitazone- and GW9662-treated mice after PH. Scale bar: 200  $\mu$ m. **(E)** Assessment of Cyclin D1 protein expression in the regenerating liver. Left panel: Western blot analysis of Cyclin D1 in untreated mice vs. rosiglitazone-treated mice. Right panel: Untreated mice vs. GW9662-treated mice. **(F)** Quantification of Western blot analysis for Cyclin D1 expression after analysis of three biological triplicates. **(G)** Real-time PCR analysis of Cyclin D1 mRNA expression after PH in untreated, rosiglitazone-treated, and GW9662-treated groups. \* $p < 0.05$ .

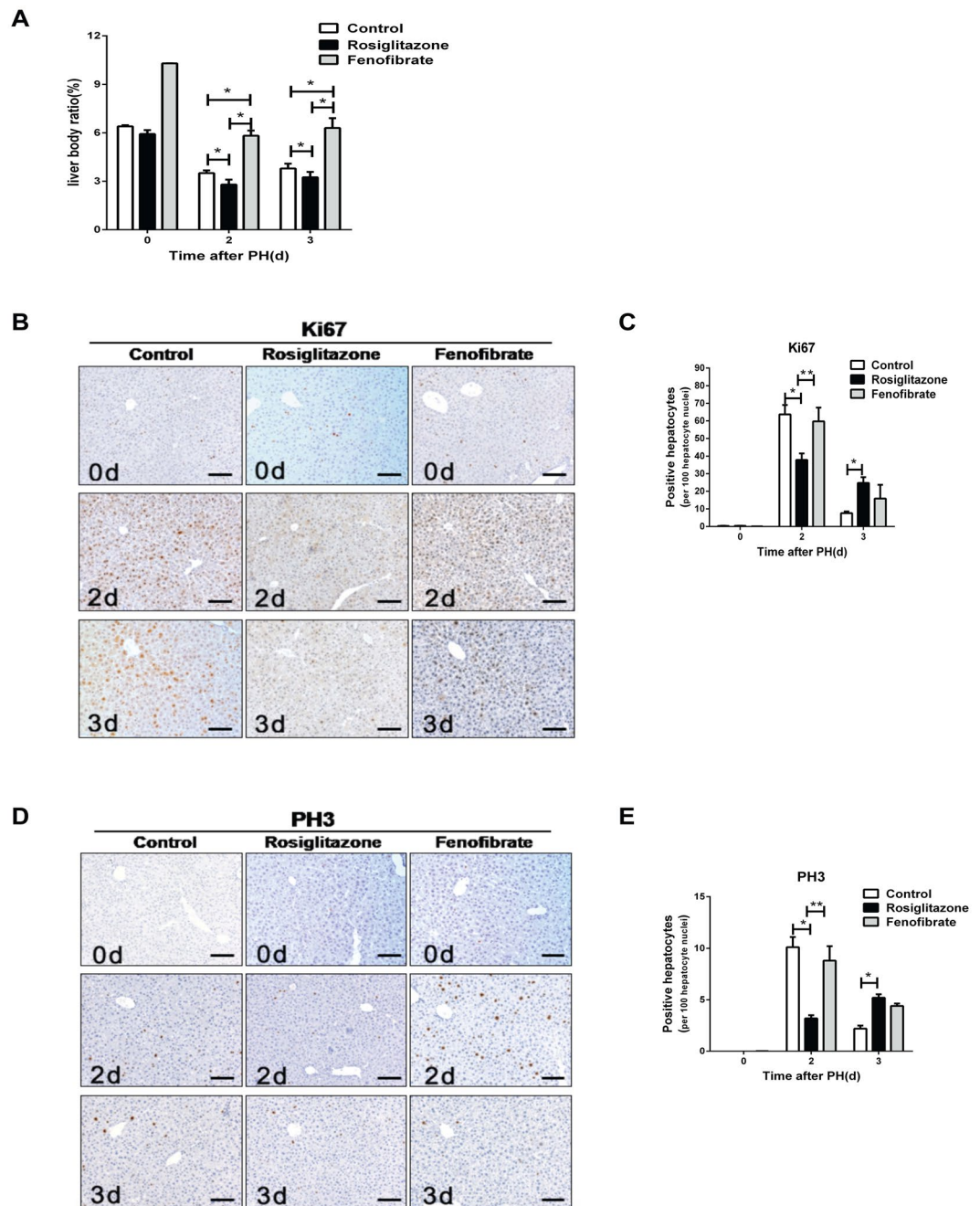


**Figure 3.** PPAR $\alpha$  activation does not influence hepatic regeneration following partial hepatectomy (A) Liver to body weight ratio in untreated mice, rosiglitazone-treated mice, and fenofibrate-treated mice at different time points after PH. (B) Representative IHC pictures of hepatic Ki67 expression after PH. (C) Quantification of Ki67-positive hepatocytes. (D) Representative IHC pictures of Ki67 expression after PH. (E) Quantification of Ki67-positive hepatocytes. \* $p < 0.05$ , \*\* $p < 0.01$ .

expression and, in consequence, activation of a subset of HGF-induced signaling events occurs that are known to inhibit hepatocyte proliferation.

**Inhibition of c-Met abrogates GW9662-induced liver regeneration and hepatocyte proliferation.** To further confirm that PPAR $\gamma$  inhibits liver regeneration via HGF/c-Met/ERK1/2 signaling pathways, we investigated whether PPAR $\gamma$  antagonist treatment is able to augment liver regeneration after blockage of c-Met activation using SGX523 by oral gavage. We observed that phosphorylation of c-Met was significantly decreased in SGX523-treated mice compared to untreated mice ( $p < 0.05$ , Fig. 5A). A significantly higher liver to body weight ratio was observed in GW9662-treated mice compared to SGX523 plus GW9662-treated mice ( $p < 0.05$ ) or SGX523-treated mice at 3 days post-PH ( $p < 0.01$ , Fig. 5B). In addition, significantly increased

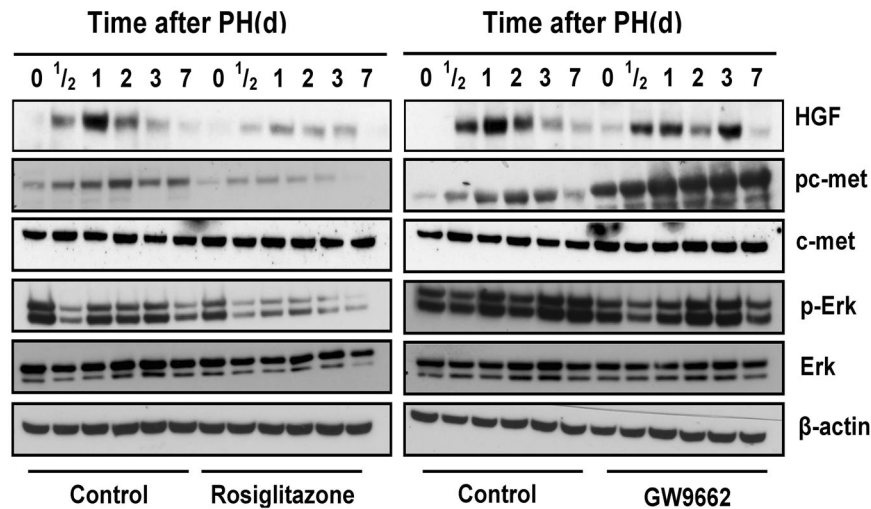


**Figure 4.** PPAR $\gamma$  inhibits the activation of HGF/c-Met/ERK1/2 signaling pathways in the regenerating liver. Hepatic expression of HGF/c-Met signaling pathway after PH in untreated vs. rosiglitazone-treated mice. Hepatic expression of HGF/c-Met signaling pathway after PH in control vs. GW9662-treated mice. The immunoblots are representative of minimum 3 biological replicates for each time point.

numbers of Ki67- and PH3-positive hepatocytes were found in GW9662-treated mice compared to SGX523 plus GW9662-treated mice ( $p < 0.01$ ) or SGX523-treated mice at 2 days post-PH ( $p < 0.001$ , Fig. 5C,D). In addition, comparison of liver to body weight ratio and numbers of Ki67- and PH3-positive hepatocytes between SGX523 plus GW9662-treated and SGX523-treated mice showed no difference neither at 2 nor at 3 days post-PH (Fig. 5B–D). These findings demonstrate that blockage of c-Met activation attenuates the effect of the PPAR $\gamma$  antagonist GW9662 on promoting a subset of HGF-induced signaling pathways, which further validates that PPAR $\gamma$  controls liver regeneration by regulating HGF/c-Met signaling in partial hepatectomized mice.

## Discussion

Liver regeneration after surgical resection or injury is a complex phenomenon, which involves numerous cytokin- and growth factor-mediated pathways, including TNF $\alpha$ , IL6, EGF, IL1, TGF $\beta$ , HGF<sup>20</sup>. As a ligand-dependent transcription factor, PPAR $\gamma$  has a cross-talk effect with the above pathways and is involved in the regulation of adipogenesis, immune response, insulin sensitivity, and glucose homeostasis<sup>21</sup>. Several studies were performed to investigate the role of PPAR $\gamma$  expression on hepatocellular proliferation during mouse liver regeneration and showed a negatively regulated effect. Furthermore, Gazit *et al.* reported an accelerated regenerative response in liver-specific PPAR $\gamma$  null mice while augmented PPAR $\gamma$  expression in fatty liver mediate the impaired regenerative response. However, a specific mechanism of PPAR $\gamma$  for liver regeneration was not displayed. In the present study, we determined the role of altered activation of hepatic PPAR $\gamma$  in regulating liver regeneration. Consistent with previous studies, our results further confirm that ligand activation of PPAR $\gamma$  by rosiglitazone inhibits liver regeneration, while the restoration of the liver tissue is significantly accelerated after treatment with the PPAR $\gamma$  antagonist GW9662 (Fig. 1A–E).

Previous studies have shown that PPAR $\gamma$  inhibits cell proliferation through cell cycle arrest at the G1/S checkpoint in hepatic oval cells, human pancreatic carcinoma cells, vascular smooth muscle cells, or induces apoptosis in malignant or non-malignant tissue<sup>22–26</sup>. Not surprisingly, we were able to show that the induction of hepatic cyclin D1/cyclin B1 expression after PH was delayed by about 12 hours after the activation of PPAR $\gamma$  by rosiglitazone (Fig. 2E–G and Supplementary Figure 1). Proliferation of hepatocytes was also decreased in the S and M phase and delayed in agonist-treated mice, while proliferation was significantly increased after antagonist treatment (Fig. 2B–D). Taken together, these data suggest that PPAR $\gamma$  inhibits hepatocyte proliferation at least partly through regulating initial cell cycle progression.

Given that PPAR $\gamma$  has multiple, interconnective cross-talks with cytokin- and growth-factor-mediated pathways associated with liver regeneration, we performed a pathway analysis to further address the underlying molecular mechanisms of PPAR $\gamma$  that inhibit liver regeneration. In this context, TNF $\alpha$ /IL6 pathways were considered as the most important pathways to direct an immediate-early gene expression and to derive cell proliferation during the initial phase of liver regeneration. Since several studies showed a negative feedback relationship between the activation of PPAR $\gamma$  and TNF $\alpha$  expression, we expected a regulatory activation of TNF $\alpha$ /IL6 pathways among untreated mice, rosiglitazone-treated, or GW9662-treated mice through an early regenerative response to PH<sup>27</sup>. Contrarily, despite the observation that all three groups produced more TNF $\alpha$ /IL6 12 hours post-PH than at the baseline, no significant differences were found in presence of the PPAR $\gamma$  agonist or antagonist at any time point (Supplementary Figure 3A–D). These findings suggest that TNF $\alpha$ /IL6-dependent hepatocyte priming is not affected by altered activation of PPAR $\gamma$  in liver regeneration induced by PH. Additionally, it is noteworthy that minimal IL6 is sufficient to achieve complete liver regeneration, which has been proved in MyD88 knockout mice using the PH model (own unpublished data).

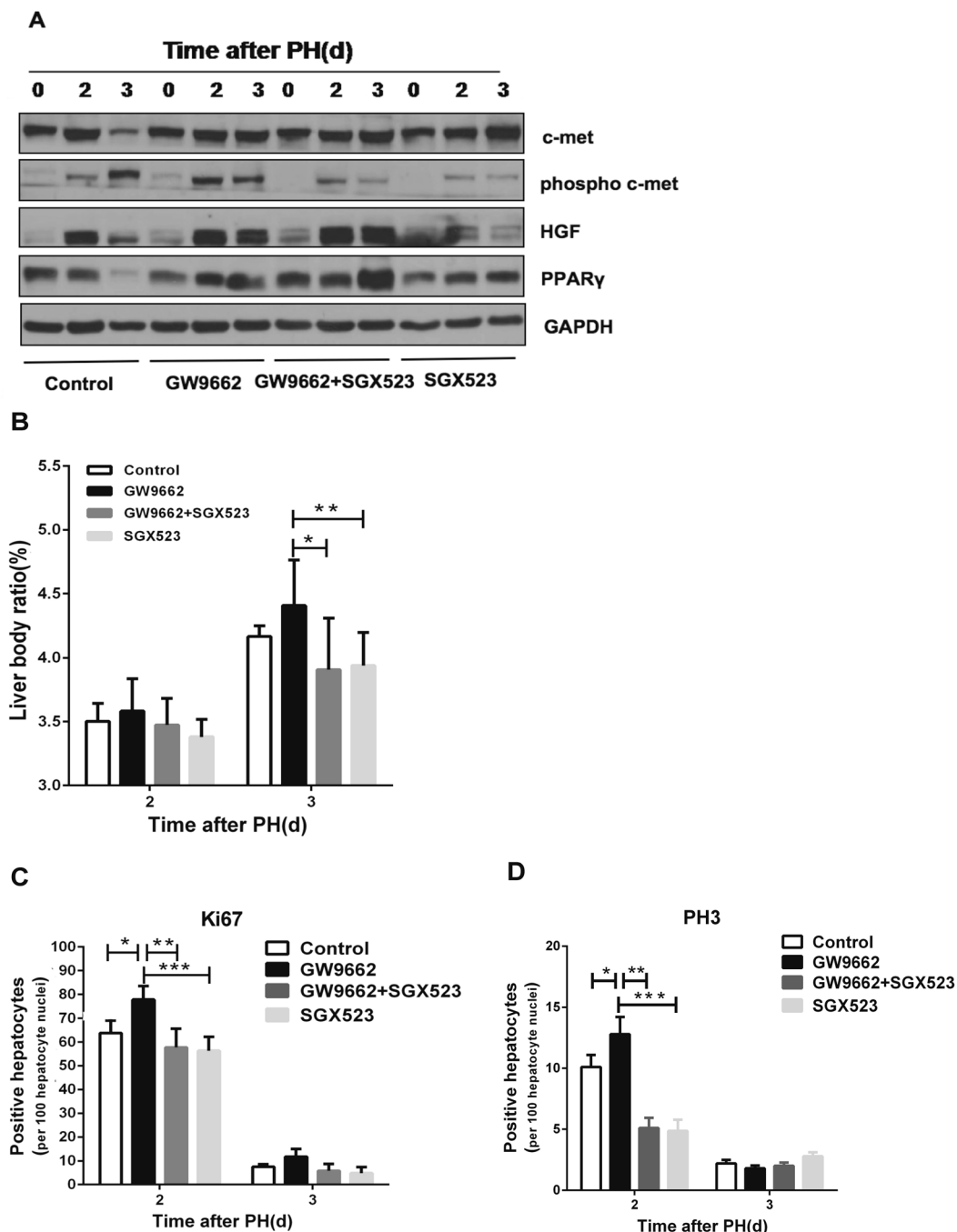


**Figure 5.** Inhibition of c-Met abrogates GW9662-induced liver regeneration and hepatocyte proliferation (A) Protein expression of PPAR $\gamma$ , HGF/c-met signaling pathway in untreated mice, GW9662-treated mice, GW9662 plus SGX523-treated mice, and SGX523-treated mice at 0, 2, and 3 days after PH. (B) Liver to body weight ratio in control mice, GW9662-treated mice, GW9665 plus SGX523-treated mice, and SGX523-treated mice at 0, 2, and 3 days after PH. (C) Quantification of hepatic Ki67 expression and (D) PH3 expression after PH. \* $p < 0.05$ , \*\* $p < 0.01$ , \*\*\* $p < 0.001$ .

Following PH, hepatic stellate cells are activated to produce hepatocyte growth factor (HGF) and integrate multiple signals to induce hepatocyte proliferation. In particular, HGF has been demonstrated to be the most important hepatocyte mitogen contributing to liver regeneration and reparation after liver injury<sup>28</sup>. HGF protein levels in plasma and the activation of its receptor c-Met are increased immediately after PH in the rat, HGF overexpression or application of exogenous HGF may induce hepatocyte proliferation and accelerate the process of liver regeneration following PH in mice<sup>29–35</sup>. When HGF and c-Met are silenced *in vivo* by RNA interference, liver regeneration is impaired and the expression pattern in many cell cycle- and apoptosis-related genes is abnormal<sup>36</sup>. Up to now, no sufficient study analyzed in particular the relationship between PPAR $\gamma$  and HGF/c-Met signaling

pathways in liver regeneration. Previous studies showed that PPAR $\gamma$  activation by telmisartan exhibited renal protective action in mice with renal atrophy and fibrosis and this prevention by telmisartan is associated with a significantly increased renal HGF expression but attenuated by GW9662<sup>27</sup>. The mechanism is that PPAR $\gamma$  mediates transcriptional upregulation of the HGF gene promoter via a novel composite cis-acting element<sup>38</sup>. Thus, HGF acts as one of the positively regulated downstream effectors of PPAR $\gamma$ . Our findings show that hepatic HGF levels are significantly downregulated after PPAR $\gamma$ -activating rosiglitazone treatment and that HGF levels are upregulated when PPAR $\gamma$  is inhibited by GW9662 (Fig. 4).

Various studies have shown that PPAR $\gamma$  is one of the downstream effectors and that activation of the ERK1/2 cascade can phosphorylate and thereby inhibit PPAR $\gamma$  activity<sup>39–41</sup>. In addition, PPAR $\gamma$  phosphorylation by activation of the ERK1/2 cascade is assumed to be more prone to ubiquitination and subsequent degradation by the proteasome<sup>42–44</sup>. In the present study, our observations revealed that hepatic phosphorylated ERK1/2 protein levels are downregulated when PPAR $\gamma$  is activated by rosiglitazone. This interesting finding not only indicates that PPAR $\gamma$  inhibits mouse liver regeneration after PH via HGF/c-Met/ERK1/2 pathways but also provides new evidence that PPAR $\gamma$  can also negatively regulate the phosphorylation of ERK1/2. The interaction between PPAR $\gamma$  and the ERK1/2 cascade is of special importance in this context. In addition, our experiments reveal that HGF/c-Met signaling pathways are blocked by SGX523 and that the accelerative action for liver regeneration by GW9662 is attenuated (Fig. 5A–D). These results further confirm that PPAR $\gamma$  inhibits mouse liver regeneration by inhibition of HGF/c-Met/ERK1/2 pathways.

In summary, our results suggest a new concept of PPAR $\gamma$  regulating liver growth and hepatocellular proliferation by inhibiting HGF/c-Met/ERK1/2 signaling pathways. Accordingly, blocking activation of c-Met attenuates PPAR $\gamma$  antagonist-induced accelerated proliferation. These findings provide additional new insights on the role of PPAR $\gamma$  during liver regeneration in response to liver resection or injury.

## References

1. Fausto, N., Campbell, J. S. & Riehle, K. J. Liver regeneration. *Hepatology* **43**, S45–53, <https://doi.org/10.1002/hep.20969> (2006).
2. Malato, Y. *et al.* Hepatocyte-specific inhibitor-of-kappaB-kinase deletion triggers the innate immune response and promotes earlier cell proliferation during liver regeneration. *Hepatology* **47**, 2036–2050, <https://doi.org/10.1002/hep.22264> (2008).
3. Michalopoulos, G. K. & DeFrances, M. C. Liver regeneration. *Science* **276**, 60–66 (1997).
4. Sakamoto, T. *et al.* Mitosis and apoptosis in the liver of interleukin-6-deficient mice after partial hepatectomy. *Hepatology* **29**, 403–411, <https://doi.org/10.1002/hep.510290244> (1999).
5. Dreyer, C. *et al.* Control of the peroxisomal beta-oxidation pathway by a novel family of nuclear hormone receptors. *Cell* **68**, 879–887 (1992).
6. Chang, T. H. & Szabo, E. Induction of differentiation and apoptosis by ligands of peroxisome proliferator-activated receptor gamma in non-small cell lung cancer. *Cancer Res* **60**, 1129–1138 (2000).
7. Kersten, S., Desvergne, B. & Wahli, W. Roles of PPARs in health and disease. *Nature* **405**, 421–424, <https://doi.org/10.1038/35013000> (2000).
8. Lehrke, M. & Lazar, M. A. The many faces of PPARgamma. *Cell* **123**, 993–999, <https://doi.org/10.1016/j.cell.2005.11.026> (2005).
9. Heaney, A. P., Fernando, M. & Melmed, S. PPAR-gamma receptor ligands: novel therapy for pituitary adenomas. *J Clin Invest* **111**, 1381–1388, <https://doi.org/10.1172/JCI16575> (2003).
10. Koga, H. *et al.* Involvement of p21(WAF1/Cip1), p27(Kip1), and p18(INK4c) in troglitazone-induced cell-cycle arrest in human hepatoma cell lines. *Hepatology* **33**, 1087–1097, <https://doi.org/10.1053/jhep.2001.24024> (2001).
11. Michalik, L. & Wahli, W. Involvement of PPAR nuclear receptors in tissue injury and wound repair. *J Clin Invest* **116**, 598–606, <https://doi.org/10.1172/JCI27958> (2006).
12. Schaefer, K. L. *et al.* Peroxisome proliferator-activated receptor gamma inhibition prevents adhesion to the extracellular matrix and induces anoikis in hepatocellular carcinoma cells. *Cancer Res* **65**, 2251–2259, <https://doi.org/10.1158/0008-5472.CAN-04-3037> (2005).
13. Turmelle, Y. P. *et al.* Rosiglitazone inhibits mouse liver regeneration. *FASEB J* **20**, 2609–2611, <https://doi.org/10.1096/fj.06-6511fj> (2006).
14. Yamamoto, Y. *et al.* Role of peroxisome proliferator-activated receptor-gamma (PPARgamma) during liver regeneration in rats. *J Gastroenterol Hepatol* **23**, 930–937, <https://doi.org/10.1111/j.1440-1746.2008.05370.x> (2008).
15. Gazit, V., Huang, J., Weymann, A. & Rudnick, D. A. Analysis of the role of hepatic PPARgamma expression during mouse liver regeneration. *Hepatology* **56**, 1489–1498, <https://doi.org/10.1002/hep.25880> (2012).
16. Mitchell, C. & Willenbring, H. A reproducible and well-tolerated method for 2/3 partial hepatectomy in mice. *Nat Protoc* **3**, 1167–1170, <https://doi.org/10.1038/nprot.2008.80> (2008).
17. Espeillac, C. *et al.* S6 kinase 1 is required for rapamycin-sensitive liver proliferation after mouse hepatectomy. *J Clin Invest* **121**, 2821–2832, <https://doi.org/10.1172/JCI44203> (2011).
18. Chiang, M. C., Cheng, Y. C., Lin, K. H. & Yen, C. H. PPARgamma regulates the mitochondrial dysfunction in human neural stem cells with tumor necrosis factor alpha. *Neuroscience* **229**, 118–129, <https://doi.org/10.1016/j.neuroscience.2012.11.003> (2013).
19. Ishii, T. *et al.* Hepatocyte growth factor stimulates liver regeneration and elevates blood protein level in normal and partially hepatectomized rats. *J Biochem* **117**, 1105–1112 (1995).
20. Taub, R. Liver regeneration: from myth to mechanism. *Nat Rev Mol Cell Biol* **5**, 836–847, <https://doi.org/10.1038/nrm1489> (2004).
21. Ahmadian, M. *et al.* PPARgamma signaling and metabolism: the good, the bad and the future. *Nat Med* **19**, 557–566, <https://doi.org/10.1038/nm.3159> (2013).
22. Cheng, J. *et al.* Peroxisome proliferator-activated receptor gamma ligands, 15-deoxy-Delta12,14-prostaglandin J2, and ciglitazone, induce growth inhibition and cell cycle arrest in hepatic oval cells. *Biochem Biophys Res Commun* **322**, 458–464, <https://doi.org/10.1016/j.bbrc.2004.07.133> (2004).
23. Motomura, W., Okumura, T., Takahashi, N., Obara, T. & Kohgo, Y. Activation of peroxisome proliferator-activated receptor gamma by troglitazone inhibits cell growth through the increase of p27KIP1 in human. Pancreatic carcinoma cells. *Cancer Res* **60**, 5558–5564 (2000).
24. Wakino, S. *et al.* Peroxisome proliferator-activated receptor gamma ligands inhibit retinoblastoma phosphorylation and G1-> S transition in vascular smooth muscle cells. *J Biol Chem* **275**, 22435–22441, <https://doi.org/10.1074/jbc.M910452199> (2000).
25. Yang, F. G. *et al.* Peroxisome proliferator-activated receptor gamma ligands induce cell cycle arrest and apoptosis in human renal carcinoma cell lines. *Acta Pharmacol Sin* **26**, 753–761, <https://doi.org/10.1111/j.1745-7254.2005.00753.x> (2005).
26. Yu, J. *et al.* Inhibitory role of peroxisome proliferator-activated receptor gamma in hepatocarcinogenesis in mice and *in vitro*. *Hepatology* **51**, 2008–2019, <https://doi.org/10.1002/hep.23550> (2010).

27. Ruan, H., Pownall, H. J. & Lodish, H. F. Troglitazone antagonizes tumor necrosis factor- $\alpha$ -induced reprogramming of adipocyte gene expression by inhibiting the transcriptional regulatory functions of NF- $\kappa$ B. *J Biol Chem* **278**, 28181–28192, <https://doi.org/10.1074/jbc.M303141200> (2003).
28. Huh, C. G. *et al.* Hepatocyte growth factor/c-met signaling pathway is required for efficient liver regeneration and repair. *Proc Natl Acad Sci USA* **101**, 4477–4482, <https://doi.org/10.1073/pnas.0306068101> (2004).
29. Bell, A., Chen, Q., DeFrances, M. C., Michalopoulos, G. K. & Zarnegar, R. The five amino acid-deleted isoform of hepatocyte growth factor promotes carcinogenesis in transgenic mice. *Oncogene* **18**, 887–895, <https://doi.org/10.1038/sj.onc.1202379> (1999).
30. Michalopoulos, G. K. Liver regeneration. *J Cell Physiol* **213**, 286–300, <https://doi.org/10.1002/jcp.21172> (2007).
31. Patijn, G. A., Lieber, A., Schowalter, D. B., Schwall, R. & Kay, M. A. Hepatocyte growth factor induces hepatocyte proliferation *in vivo* and allows for efficient retroviral-mediated gene transfer in mice. *Hepatology* **28**, 707–716, <https://doi.org/10.1002/hep.510280317> (1998).
32. Pediaditakis, P., Lopez-Talavera, J. C., Petersen, B., Monga, S. P. & Michalopoulos, G. K. The processing and utilization of hepatocyte growth factor/scatter factor following partial hepatectomy in the rat. *Hepatology* **34**, 688–693, <https://doi.org/10.1053/jhep.2001.27811> (2001).
33. Sakata, H. *et al.* Hepatocyte growth factor/scatter factor overexpression induces growth, abnormal development, and tumor formation in transgenic mouse livers. *Cell Growth Differ* **7**, 1513–1523 (1996).
34. Shiota, G. & Kawasaki, H. Hepatocyte growth factor in transgenic mice. *Int J Exp Pathol* **79**, 267–277 (1998).
35. Stolz, D. B., Mars, W. M., Petersen, B. E., Kim, T. H. & Michalopoulos, G. K. Growth factor signal transduction immediately after two-thirds partial hepatectomy in the rat. *Cancer Res* **59**, 3954–3960 (1999).
36. Paranjpe, S. *et al.* Cell cycle effects resulting from inhibition of hepatocyte growth factor and its receptor c-Met in regenerating rat livers by RNA interference. *Hepatology* **45**, 1471–1477, <https://doi.org/10.1002/hep.21570> (2007).
37. Kusunoki, H. *et al.* Telmisartan exerts renoprotective actions via peroxisome proliferator-activated receptor- $\gamma$ /hepatocyte growth factor pathway independent of angiotensin II type 1 receptor blockade. *Hypertension* **59**, 308–316, <https://doi.org/10.1161/HYPERTENSIONAHA.111.176263> (2012).
38. Jiang, J. G., Johnson, C. & Zarnegar, R. Peroxisome proliferator-activated receptor  $\gamma$ -mediated transcriptional up-regulation of the hepatocyte growth factor gene promoter via a novel composite cis-acting element. *J Biol Chem* **276**, 25049–25056, <https://doi.org/10.1074/jbc.M101611200> (2001).
39. Adams, M., Reginato, M. J., Shao, D., Lazar, M. A. & Chatterjee, V. K. Transcriptional activation by peroxisome proliferator-activated receptor  $\gamma$  is inhibited by phosphorylation at a consensus mitogen-activated protein kinase site. *J Biol Chem* **272**, 5128–5132 (1997).
40. Diradourian, C., Girard, J. & Pegorier, J. P. Phosphorylation of PPARs: from molecular characterization to physiological relevance. *Biochimie* **87**, 33–38, <https://doi.org/10.1016/j.biochi.2004.11.010> (2005).
41. Hu, E., Kim, J. B., Sarraf, P. & Spiegelman, B. M. Inhibition of adipogenesis through MAP kinase-mediated phosphorylation of PPAR $\gamma$ . *Science* **274**, 2100–2103 (1996).
42. Burns, K. A. & Vanden Heuvel, J. P. Modulation of PPAR activity via phosphorylation. *Biochim Biophys Acta* **1771**, 952–960, <https://doi.org/10.1016/j.bbali.2007.04.018> (2007).
43. Genini, D. & Catapano, C. V. Control of peroxisome proliferator-activated receptor fate by the ubiquitin-proteasome system. *J Recept Signal Transduct Res* **26**, 679–692, <https://doi.org/10.1080/10799890600928202> (2006).
44. Hosooka, T. *et al.* Dok1 mediates high-fat diet-induced adipocyte hypertrophy and obesity through modulation of PPAR- $\gamma$  phosphorylation. *Nat Med* **14**, 188–193, <https://doi.org/10.1038/nm1706> (2008).

## Author Contributions

Conceptualization (C.W.M., J.K., D.H. and N.H. formulated the research goals and aims.), Analysis (Z.C., L.L., X.Z. and M.L. applied statistical techniques to analyse the study data.), Funding acquisition (C.W.M., J.K., H.F., D.H. and N.H. acquired financial support for the project.), Investigation (Z.C., L.L., X.Z., M.L., Y.W., V.A. and M.L. performed the experiments and data collection.), Supervision (G.v.F., Y.S., C.W.M., J.K., H.F., D.H. and N.H. supervised the project.), Visualization (Z.C., L.L., X.Z., M.L., Y.W., G.v.F., D.H. and N.H. prepared, created and visualized the data.), Writing original draft (Z.C., L.L., V.A., M.L., G.v.F., Y.S., D.H. and N.H. prepared, wrote, and reviewed the manuscript).

## Additional Information

**Supplementary information** accompanies this paper at <https://doi.org/10.1038/s41598-018-30426-5>.

**Competing Interests:** The authors declare no competing interests.

**Publisher's note:** Springer Nature remains neutral with regard to jurisdictional claims in published maps and institutional affiliations.



**Open Access** This article is licensed under a Creative Commons Attribution 4.0 International License, which permits use, sharing, adaptation, distribution and reproduction in any medium or format, as long as you give appropriate credit to the original author(s) and the source, provide a link to the Creative Commons license, and indicate if changes were made. The images or other third party material in this article are included in the article's Creative Commons license, unless indicated otherwise in a credit line to the material. If material is not included in the article's Creative Commons license and your intended use is not permitted by statutory regulation or exceeds the permitted use, you will need to obtain permission directly from the copyright holder. To view a copy of this license, visit <http://creativecommons.org/licenses/by/4.0/>.

© The Author(s) 2018